Unsplit complex frequency shifted perfectly matched layer for second-order wave equation using auxiliary differential equations

Yingjie Gao,[a] Jinhai Zhang, and Zhenxing Yao
Institute of Geology and Geophysics, Chinese Academy of Sciences, Beijing, China
gaoyingjie@mail.iggcas.ac.cn, zjh@mail.iggcas.ac.cn, yaozx@mail.iggcas.ac.cn

Abstract: The complex frequency shifted perfectly matched layer (CFS-PML) can improve the absorbing performance of PML for nearly grazing incident waves. However, traditional PML and CFS-PML are based on first-order wave equations; thus, they are not suitable for second-order wave equation. In this paper, an implementation of CFS-PML for second-order wave equation is presented using auxiliary differential equations. This method is free of both convolution calculations and third-order temporal derivatives. As an unsplit CFS-PML, it can reduce the nearly grazing incidence. Numerical experiments show that it has better absorption than typical PML implementations based on second-order wave equation.

Date Received: August 20, 2015 **Date Accepted:** December 8, 2015

1. Introduction

Numerical simulation is essential for understanding wave phenomena and for estimating the physical parameters of the materials. Due to the restrictions on both memory demand and computational cost, we have to introduce artificial boundaries to concentrate on the interested area of the model; however, unwanted reflections from these artificial boundaries would contaminate the wavefields and an artificial boundary condition is needed. Many methods have been proposed for this purpose as reviewed by Gao *et al.* (2016), and the perfectly matched layer (PML) (Bérenger, 1994) breaks a new way by introducing physical attenuations to the wave equation. However, traditional PML would produce apparent artificial reflections for nearly grazing incident waves, low-frequency waves, and evanescent waves (Festa and Vilotte, 2005; Komatitsch and Martin, 2007; Drossaert and Giannopoulos, 2007a). The complex frequency shifted perfectly matched layer (CFS-PML) (Kuzuoglu and Mittram, 1996) has a better absorbing performance in these cases (Festa and Vilotte, 2005; Drossaert and Giannopoulos, 2007b). In addition, traditional PML adopts a nonphysical splitting of wave equations, which have been proven to be weakly well-posed. Convolutional PML (Roden and Gedney, 2000) and auxiliary differential equation perfectly matched layer (ADE-PML) (Ramadan, 2003; Zhang and Shen, 2010) are proposed to solve this problem.

Generally, the traditional PML, CFS-PML, convolution PML, and ADE-PML are derived based on the first-order equations; thus, they cannot be directly used for the second-order wave equation. This means that the second-order wave equation must be transformed into the first-order form in order to adopt PML. In fact, the second-order wave equation is more simple and compact in form than the first-order one; thus, it is widely used for acoustics (e.g., Liu and Tao, 1997; Qi and Geers, 1998; Bonomo *et al.*, 2015) and seismic explorations. It is worthwhile to directly develop the PML for the second order wave equation.

Komatitsch and Tromp (2003) construct the PML for the second-order displacement elastic wave equation by splitting the wavefield into four terms. Third-order temporal partial derivatives arise and an auxiliary variable should be introduced to deal with this problem. Liu *et al.* (2012) implement this method in a much easier way. However, this method cannot be used in the implementation of CFS-PML for the second-order wave equation, since the coordinate stretched operator of CFS-PML is more complicated than that of the PML. Li and Matar (2010) propose an implementation of CFS-PML for the second-order elastic wave equations; whereas, the temporal

[a]Also at: University of Chinese Academy of Sciences, Beijing, China. Author to whom correspondence should be addressed.

partial derivative is in the second order but the spatial partial derivatives are still in the first order. It is difficult to extend this method to the second-order wave equation. Recently, Ping *et al.* (2014) presented a split PML for the second-order elastic wave equation.

Pasalic and McGarry (2010) propose an implementation of unsplit CFS-PML for the second-order wave equation using a convolutional algorithm (Roden and Gedney, 2000). However, this method introduces additional convolution and thus would be too complicated in implementation. Ma *et al.* (2013, 2014) propose a new kind of ADE-PML for the second-order wave equation, which involves neither convolution nor third-order temporal derivatives; thus, it is pretty direct in implementation. As a result, the storage requirement and computational cost are apparently lower than that of split PML (e.g., Komatitsch and Tromp, 2003; Ping *et al.*, 2014). In this paper, we extend the ADE-PML proposed by Ma *et al.* (2013, 2014) to the unsplit CFS-PML for the second-order wave equation. Compared with the ADE-PML proposed by Ma *et al.* (2013, 2014), our method can greatly reduce the nearly grazing incidence reflections due to using CFS.

2. CFS-PML for the second-order wave equation

The second-order wave equation in the frequency domain is

$$\frac{\partial^2 U}{\partial x^2}+\frac{\partial^2 U}{\partial z^2}=\frac{(j\omega)^2}{v^2}U, \tag{1}$$

where $U \equiv U(x,z;\omega)$ is the Fourier transform of the pressure $u \equiv u(x,z;t)$, $j=\sqrt{-1}$, ω is the circular frequency, and v is the velocity (or wave speed). For simplicity, we only consider the x-direction. The wave equation can be extended to complex coordinates as follows:

$$s(x)=\chi(x)+\frac{d(x)}{\alpha(x)+j\omega}, \tag{2}$$

thus, we have

$$\frac{\partial}{\partial x}\rightarrow\frac{\partial}{\partial \tilde{x}}=\frac{1}{s}\frac{\partial}{\partial x}, \tag{3}$$

where $s(x)$ is the complex stretching function and $d(x)$ is the attenuation coefficient. Parameters $d(x)$, $\alpha(x)$, and $\chi(x)$ are expressed as follows:

$$d(x)=d_0\left(\frac{x}{\delta}\right)^{p_d}, \tag{4}$$

$$\chi=1+(\chi_{\max}-1)\left(\frac{x}{\delta}\right)^{p_\chi}, \tag{5}$$

$$\alpha=\alpha_{\max}\left[1-\left(\frac{x}{\delta}\right)^{p_\alpha}\right], \tag{6}$$

where $\alpha_{\max}=\pi f_0$, f_0 is the dominant frequency of the source time function, δ is the width of the PML, and x is the distance to the innermost layer of the PML. The parameters p_d, p_χ, and p_α typically range from 1 to 4 and 2 is commonly used (Roden and Gedney, 2000; Zhang and Shen, 2010). We use $p_d=2$, $p_\chi=2$, and $p_\alpha=1$ as suggested by Zhang and Shen (2010) and $d_0=[(p_d+1)v_{\max}\ln(1/R)]/(2\delta)$ by Collino and Tsogka (2001), where $v_{\max}$ is the maximum velocity and R is the theoretical reflection coefficient. For a PML width of N number of cells, R can be expressed as $\log_{10}(R)=[-(\log_{10}(N)-1)/\log_{10}(2)]-3$. Generally $\chi_x=1$ is good enough for most applications (Komatitsch and Martin, 2007); thus, Eq. (2) becomes $s=1+d/(\alpha+j\omega)$. With the stretched complex coordinates, Eq. (1) can be expressed as

$$\frac{-\omega^2}{v^2}U=\frac{\partial^2 U}{\partial \tilde{x}^2}+\frac{\partial^2 U}{\partial z^2}=\frac{1}{s}\frac{\partial}{\partial x}\left(\frac{1}{s}\frac{\partial U}{\partial x}\right)+\frac{\partial^2 U}{\partial z^2}. \tag{7}$$

Equation (7) is the CFS-PML in the x-direction. We can obtain a similar equation in the z-direction by exchanging the variables x and z for all related terms.

3. CFS-PML using ADE

We apply the ADE proposed by Ma *et al.* (2013, 2014) to reduce the artificial reflections associated with nearly grazing incidence when solving the second-order wave equation with the CFS-PML. The stretched term along the x-direction in Eq. (7) can be expressed as

$$\begin{aligned}\frac{1}{s}\frac{\partial}{\partial x}\left(\frac{1}{s}\frac{\partial U}{\partial x}\right) &= \frac{1}{s}\frac{\partial}{\partial x}\left(\frac{1}{s}\right)\frac{\partial U}{\partial x}+\frac{1}{s^2}\frac{\partial}{\partial x}\left(\frac{\partial U}{\partial x}\right)\\ &= -\frac{s'}{s^3}\frac{\partial U}{\partial x}+\frac{1}{s^2}\frac{\partial^2 U}{\partial x^2}\\ &= -\frac{\left[d'(\alpha+j\omega)-d\alpha'\right](\alpha+j\omega)}{(\alpha+j\omega+d)^3}\frac{\partial U}{\partial x}+\frac{(\alpha+j\omega)^2}{(\alpha+j\omega+d)^2}\frac{\partial^2 U}{\partial x^2},\end{aligned} \tag{8}$$

where a primed variable denotes its partial derivative with respect to x. Introducing a variable $p \equiv \alpha + j\omega + d$ and substituting it into Eq. (8), we can obtain

$$\begin{aligned}\frac{1}{s}\frac{\partial}{\partial x}\left(\frac{1}{s}\frac{\partial U}{\partial x}\right) &= \frac{\partial^2 U}{\partial x^2}-\left(\frac{d'}{p}\frac{\partial U}{\partial x}+\frac{2d}{p}\frac{\partial^2 U}{\partial x^2}\right)\\ &\quad +\frac{\lambda}{p^2}-\left(\frac{d^2 d'}{p^3}+\frac{d^2\alpha'}{p^3}\right)\frac{\partial U}{\partial x},\end{aligned} \tag{9}$$

where

$$\lambda \equiv 2dd'\frac{\partial U}{\partial x}+d\alpha'\frac{\partial U}{\partial x}+d^2\frac{\partial^2 U}{\partial x^2}.$$

Introducing an auxiliary

$$U_1 \equiv \left(\frac{d'}{p}\frac{\partial U}{\partial x}+\frac{2d}{p}\frac{\partial^2 U}{\partial x^2}\right)-\frac{\lambda}{p^2}+\left(\frac{d^2 d'}{p^3}+\frac{d^2\alpha'}{p^3}\right)\frac{\partial U}{\partial x}, \tag{10}$$

Eq. (7) becomes

$$\frac{-\omega^2}{v^2}U = \frac{\partial^2 U}{\partial x^2}+\frac{\partial^2 U}{\partial z^2}-U_1. \tag{11}$$

Multiplying both sides of Eq. (10) by p, we obtain

$$pU_1 = \left(d'\frac{\partial U}{\partial x}+2d\frac{\partial^2 U}{\partial x^2}\right)-U_2, \tag{12}$$

where U_2 is defined as

$$U_2 \equiv \frac{\lambda}{p}-\left(\frac{d^2 d'}{p^2}+\frac{d^2\alpha'}{p^2}\right)\frac{\partial U}{\partial x}. \tag{13}$$

Multiplying both sides of Eq. (13) by p, we obtain

$$pU_2 = \lambda - U_3, \tag{14}$$

where U_3 is defined as

$$U_3 \equiv \left(\frac{d^2 d'}{p}+\frac{d^2\alpha'}{p}\right)\frac{\partial U}{\partial x}. \tag{15}$$

Multiplying both sides of Eq. (15) by p, we obtain

$$pU_3 = (d^2 d'+d^2\alpha')\frac{\partial U}{\partial x}. \tag{16}$$

Substituting $p \equiv \alpha + j\omega + d$ into Eqs. (11), (12), (14), and (16), we can obtain the following frequency-domain equations in Cartesian coordinates:

$$
\begin{aligned}
&(\alpha + j\omega + d)U_3 = d^2(d' + \alpha')\frac{\partial U}{\partial x},\\
&(\alpha + j\omega + d)U_2 = d\left(2d'\frac{\partial U}{\partial x} + \alpha'\frac{\partial U}{\partial x} + d\frac{\partial^2 U}{\partial x^2}\right) - U_3,\\
&(\alpha + j\omega + d)U_1 = \left(d'\frac{\partial U}{\partial x} + 2d\frac{\partial^2 U}{\partial x^2}\right) - U_2,\\
&\frac{-\omega^2}{v^2}U = \frac{\partial^2 U}{\partial x^2} + \frac{\partial^2 U}{\partial z^2} - U_1.
\end{aligned} \tag{17}
$$

Transforming the above equations back to the time domain, we have

$$
\begin{aligned}
&\left(\alpha + \frac{\partial}{\partial t} + d\right)u_3 = d^2(d' + \alpha')\frac{\partial u}{\partial x},\\
&\left(\alpha + \frac{\partial}{\partial t} + d\right)u_2 = d\left(2d'\frac{\partial u}{\partial x} + \alpha'\frac{\partial u}{\partial x} + d\frac{\partial^2 u}{\partial x^2}\right) - u_3,\\
&\left(\alpha + \frac{\partial}{\partial t} + d\right)u_1 = \left(d'\frac{\partial u}{\partial x} + 2d\frac{\partial^2 u}{\partial x^2}\right) - u_2,\\
&\frac{1}{v^2}\frac{\partial^2 u}{\partial t^2} = \frac{\partial^2 u}{\partial x^2} + \frac{\partial^2 u}{\partial z^2} - u_1.
\end{aligned} \tag{18}
$$

Since u_3 depends only on u, it should be updated first; then u_2 is updated, which depends on u and u_3; next u_1 is updated, which depends on u and u_2; finally, u is updated. The similar expansion can be done in the z-direction.

Compared with the original split PML (Komatitsch and Tromp, 2003; Xing, 2010), which needs to solve three second-order and one first-order auxiliary equations, our method contains only three first-order auxiliary equations, which facilitates the implementation and can greatly reduce memory demand and computational cost simultaneously. Compared with the convolutional CFS-PML for the second-order wave equation proposed by Pasalic and McGarry (2010), our ADE-CFS-PML is free of convolution.

4. Numerical experiments

We performed several numerical experiments on a homogeneous square model. The wave velocity was 3000 m/s. The spatial grid interval was 10 m, and the grid number was 301×301. The source was a Ricker wavelet with a dominant frequency of 15 Hz. Four kinds of PML implementations were compared in order to verify the performance of the proposed method: PML for the first-order wave equations (Liu and Tao, 1997; Qi and Geers, 1998) (first-order PML for short), ADE-PML for the second-

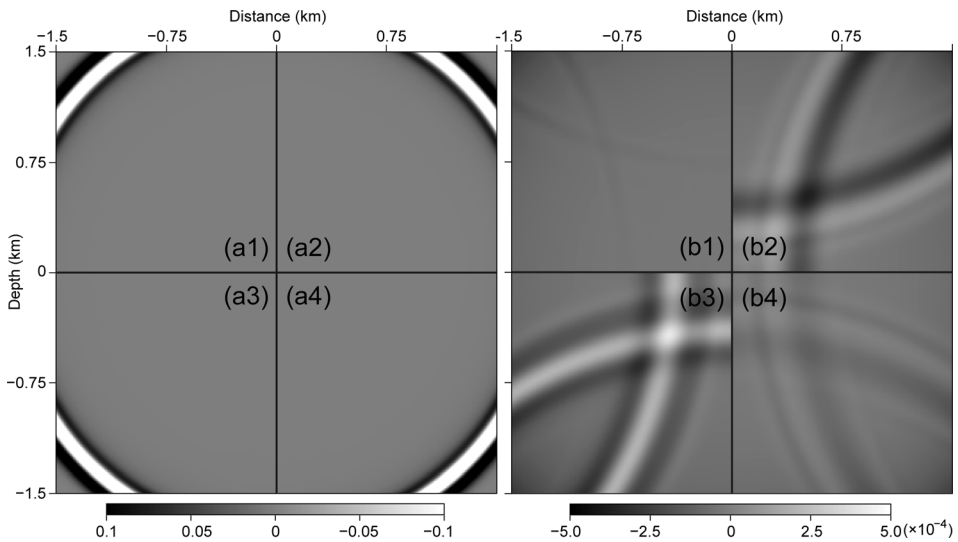

Fig. 1. Snapshots of wavefield using different boundary conditions. (a) At 750 ms and (b) at 1100 ms. (a1) First-order PML; (a2) ADE-PML; (a3) second-order PML; (a4) ADE-CFS-PML. (b1) First-order PML; (b2) ADE-PML; (b3) second-order PML; (b4) ADE-CFS-PML.

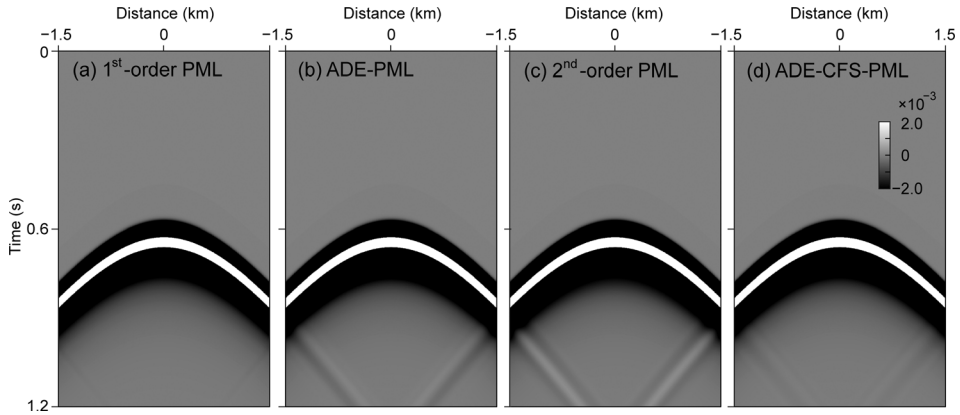

Fig. 2. Shot profiles of a point source with different absorbing boundaries. (a) First-order PML; (b) ADE-PML; (c) second-order PML; (d) ADE-CFS-PML.

order wave equation proposed by Ma *et al.* (2014), PML for the second-order wave equation proposed by Komatitsch and Tromp (2003) (second-order PML for short); and ADE-CFS-PML for the second-order equation presented here. The total number of absorbing layers was 30 for each method.

Figure 1 shows the snapshots obtained by different methods. Among the four methods listed, the absorption performance of the first-order PML was the best since it can take advantage of the staggered grid. In addition, the absorption performance of ADE-CFS-PML was better than that of either ADE-PML or second-order PML. This indicates that ADE-CFS-PML was the best absorbing boundary for the second-order wave equation. We can draw the same conclusions from the profiles recorded at the surface, as shown in Fig. 2.

In practical applications, the model was sometimes very large in scale, which would lead to nearly grazing incidence when the wavefields were propagating far away from the source. We further examined ADE-PML and ADE-CFS-PML using a long model. The grid number was 601×81. The spatial grid interval was 10 m, and the source was a Ricker wavelet with a dominant frequency of 7 Hz. The seismic source was located at 0 m along the x-direction and 100 m in depth. The wave velocity was 3000 m/s.

We used a much larger model to generate an ideal wavefield that has no boundary reflection, which can be regarded as a theoretical reference to check the performance of both ADE-PML and ADE-CFS-PML. Figure 3 shows the profiles recorded at the surface of the model. Obviously, both for the non-grazing incident waves or nearly grazing incident waves, the absorption performance of ADE-CFS-PML is better than that of ADE-PML. These numerical experiments show that both the ADE and CFS work well for the PML after we extend the ADE-PML proposed by Ma *et al.* (2013, 2014) to the CSF-PML.

For the convenience of comparing the absorption performances of different boundary conditions, we calculate the numerical reflection coefficient by

$$R_p = \left| \frac{\max(u_{\text{ref}}) - \max(u_{\text{mod}})}{\max(u_{\text{ref}})} \right|, \tag{19}$$

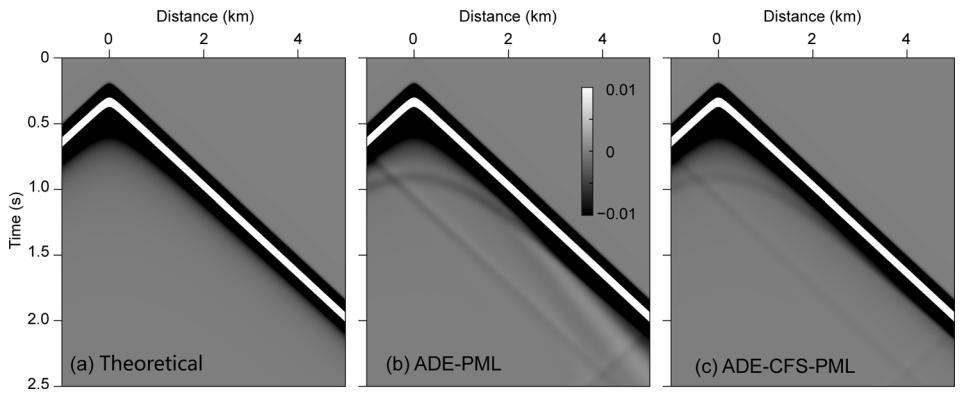

Fig. 3. Shot profiles of a point source on the surface of the long model. (a) Theoretical record; (b) ADE-PML; (c) ADE-CFS-PML.

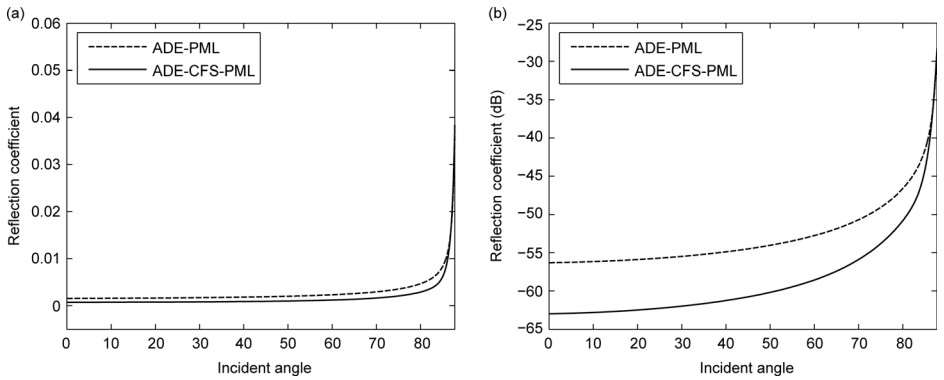

Fig. 4. Comparison of the reflection coefficient computed by numerical simulations. (a) Absolute values of numerical reflection coefficient. (b) The dB values of numerical reflection coefficient.

where u_{ref} is the theoretical wavefield without artificial reflections, and u_{mod} is the wavefield with different artificial boundary conditions. Figure 4(a) shows the numerical reflection coefficient for different boundary conditions at different incident angles, and Fig. 4(b) shows the decibel (dB) values of numerical reflection coefficient calculated by $\mathrm{dB}(R_p) = 20\log_{10}R_p$. Obviously, the ADE-CFS-PML has a better absorbing performance compared with ADE-PML for almost all incident angles, and the reflection coefficient of the ADE-CFS-PML for nearly grazing incident wave is smaller than that of ADE-PML.

5. Conclusions

We present an efficient implementation of unsplit CFS-PML using ADE for the second-order wave equation. This method does not need to split the wavefield, which eliminates solving convolution and the third-order temporal derivatives. Our method is easier to understand in form and is fairly simple in implementation. Numerical experiments show our method has better accuracy compared with typical existing PML implementations for the second-order wave equation.

Acknowledgments

We thank Youshan Liu for helpful discussions on PML implementations. This research was supported by the National Natural Science Foundation of China (Grant No. 41130418) and the National Major Project of China (Grant No. 2011ZX05008-006).

References and links

Bérenger, J. P. (**1994**). "A perfectly matched layer for the absorption of electromagnetic waves," J. Comput. Phys. **114**, 185–200.

Bonomo, A. L., Chotiros, N. P., and Isakson, M. J. (**2015**). "On the validity of the effective density fluid model as an approximation of a poroelastic sediment layer," J. Acoust. Soc. Am. **138**, 748–757.

Collino, F., and Tsogka, C. (**2001**). "Application of the perfectly matched absorbing layer model to the linear elastodynamic problem in anisotropic heterogeneous media," Geophys. **66**, 294–307.

Drossaert, F. H., and Giannopoulos, A. (**2007a**). "A nonsplit complex frequency-shifted PML based on recursive integration for FDTD modeling of elastic waves," Geophys. **72**, T9–T17.

Drossaert, F. H., and Giannopoulos, A. (**2007b**). "Complex frequency shifted convolution PML for FDTD modelling of elastic waves," Wave Motion **44**, 593–604.

Festa, G., and Vilotte, J.-P. (**2005**). "The Newmark scheme as velocity–stress time-staggering: An efficient PML implementation for spectral element simulations of elastodynamics," Geophys. J. Int. **161**, 789–812.

Gao, Y., Song, H., Zhang, J., and Yao, Z. (**2016**). "Comparison of artificial absorbing boundaries for acoustic wave equation modeling," Explor. Geophys. (in press).

Komatitsch, D., and Martin, R. (**2007**). "An unsplit convolutional perfectly matched layer improved at grazing incidence for the seismic wave equation," Geophys. **72**, SM155–SM167.

Komatitsch, D., and Tromp, J. (**2003**). "A perfectly matched layer absorbing boundary condition for the second-order seismic wave equation," Geophys. J. Int. **154**, 146–153

Kuzuoglu, M., and Mittra, R. (**1996**). "Frequency dependence of the constitutive parameters of causal perfectly matched anisotropic absorbers," IEEE Microw. Guided Wave Lett. **6**, 447–449.

Li, Y., and Matar, O. B. (**2010**). "Convolutional perfectly matched layer for elastic second-order wave equation," J. Acoust. Soc. Am. **127**, 1318–1327.

Liu, Q., and Tao, J. (**1997**). "The perfectly matched layer for acoustic waves in absorptive media," J. Acoust. Soc. Am. **102**, 2072–2082.

Liu, Y., Liu, S., Zhang, M., and Ma, D. (**2012**). "An improved perfectly matched layer absorbing boundary condition for second order elastic wave equation," Prog. Geophys. (in Chinese) **27**, 2113–2122.

Ma, Y., Yu, J., and Wang, Y. (**2013**). "Unsplit perfectly matched layer for second-order acoustic wave equation," Acta Acustica (in Chinese) **38**, 681–686.

Ma, Y., Yu, J., and Wang, Y. (**2014**). "A novel unsplit perfectly matched layer for the second-order acoustic wave equation," Ultrasonics **54**, 1568–1574.

Pasalic, D., and McGarry, R. (**2010**). "Convolutional perfectly matched layer for isotropic and anisotropic acoustic wave equations," in 2010 SEG Annual Meeting (Society of Exploration Geophysicists).

Ping, P., Zhang, Y., and Xu, Y. (**2014**). "A multiaxial perfectly matched layer (M-PML) for the long-time simulation of elastic wave propagation in the second-order equations," J. Appl. Geophys. **101**, 124–135.

Qi, Q., and Geers, T. L. (**1998**). "Evaluation of the perfectly matched layer for computational acoustics," J. Comput. Phys. **139**, 166–183.

Ramadan, O. (**2003**), "Auxiliary differential equation formulation: An efficient implementation of the perfectly matched layer," IEEE Microwave Wireless Components Lett. **13**(2), 69–71.

Roden, J. A., and Gedney, S. D. (**2000**). "Convolutional PML (CPML): An efficient FDTD implementation of the CFS-PML for arbitrary media," Micro. Opt. Tech. Lett. **27**, 334–338.

Xing, L. (**2010**). "PML condition for the numerical simulation of acoustic wave," in *2010 International Conference on Computing, Control and Industrial Engineering (CCIE)*, Wuhan, pp. 129–132.

Zhang, W., and Shen, Y. (**2010**). "Unsplit complex frequency-shifted PML implementation using auxiliary differential equations for seismic wave modeling," Geophys. **75**, T141–T154.